An NFC Air Interface coupling model for Contactless System Performance estimation

Andreas Schober*, Massimo Ciacci‡, Michael Gebhart†
* Graz University of Technology,
Email: aschober@student.tugraz.at
‡ NXP Research, Modem and Signal Processing,
Email: massimo.ciacci@nxp.com
† NXP Semiconductors Austria GmbH,
Email: michael.gebhart@nxp.com

***Abstract*—The near-field communication channel is mainly determined by the coupling of two resonant loop antennas and their HF system properties. Such properties change dynamically during operation, affecting significantly power transfer and communication performance. Both these effects are related to an impedance mismatch which arises due to a varying coupling factor. In this paper we present a Matlab-based network simulation model which allows to estimate impedance and contactless performance aspects as a function of coupling, and to determine appropriate impedance matching and antenna design parameters.**

Keywords—Near Field Communication, Inductive Coupling, Impedance Matching, Contactless Communication.

I. INTRODUCTION

Near-Field Communication (NFC) [1], the latest of the contactless communication technologies is currently attracting huge interest as a new feature for Smartphones, tablets and other mobile personal devices. About 150 million Smartphones were equipped with NFC in 2012; this is a quarter of the world-wide Smartphone market. Based on reliable contactless card technology and incorporating the main protocols used in this technology, e.g. Proximity Type A and B interface and the Japanese FeliCa protocol, NFC offers an intuitive way to open a communication link, and allows secure personal actions like payment or authentication. Product Standards like the Proximity Base Standard also specify communication properties, like modulation characteristics or alternating *H*-field strength for Proximity Integrated Circuit Cards (PICC) and Readers, called Proximity Coupling Devices (PCD). For an NFC device to be able to communicate to all devices which are fabricated according to these standards, for true interoperability, not only the protocol, but also these aspects of communication must fit to the specifications of all involved contactless standards. Unlike in other product standards, the properties for Contactless Communication Technologies are specified and tested at the Air Interface [2]. Voltages, currents and the electrical circuit for implementation are open to the manufacturing company; so different approaches may exist, which can all be standard conformant. The question of how an NFC chip together with external components like the NFC antenna and an impedance matching network will perform at the contactless interface becomes then of interest.

In this paper we present a model, which is able to answer such questions. Moreover, indicating the available RF output power and some RF system properties of a given network topology, it allows to answer questions like which is the smallest standard-conformant antenna size for a system, or the optimum *Q*-factor to choose.

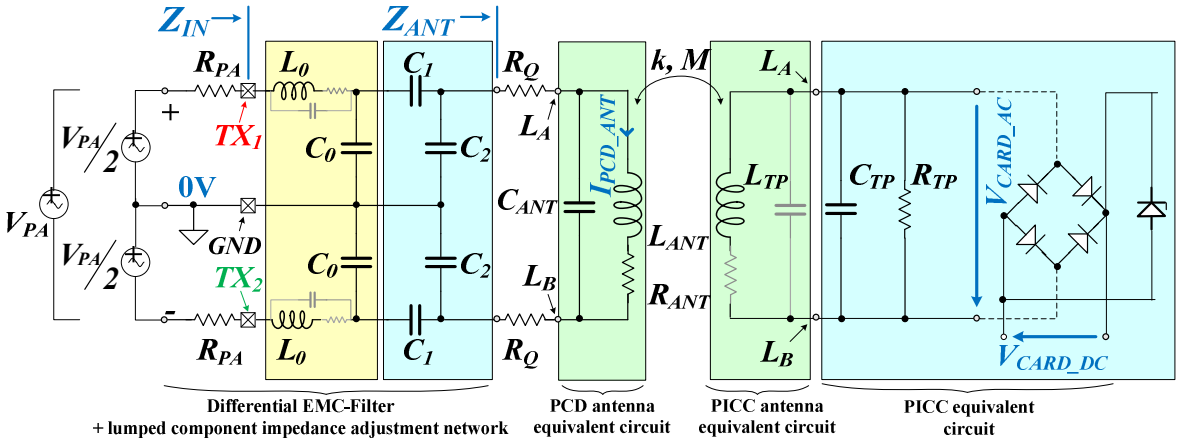

Fig. 1. Schematics of the considered NFC coupling scenario.

Our simulation model is based on complex network calculations on a linearized version of the equivalent circuit of the contactless coupling network shown in fig. 1. Implemented in a mathematical software like Matlab or MathCAD, such model is able to provide estimates very rapidly, compared to time-domain circuit simulation software like Spice or Cadence, and despite the linear approximation it proved to be sufficiently accurate for most considerations. In our contribution, we present the network equations based on classical complex network calculation, which are used as the core of the simulation model. Furthermore, we describe problems and limitations of this approach. Finally we present results for an NFC coupling scenario as function of distance, which is solved using the presented model.

II. Equivalent Circuit

The Near Field Communication (NFC) coupling system consists of a contactless HF reader and a contactless card. The electrical circuits in the card, the antenna and an integrated batteryless chip, are called transponder in this context. Relevant for coupling at the air interface is the equivalent antenna circuit for reader and transponder, furthermore on PCD side an impedance adjustment network, a so-called Electromagnetic Compatibility (EMC) filter, and the source, which is the driver amplifier output of the integrated reader chip. On transponder side, following the antenna resonant circuit there is a rectifier which provides the direct current (DC) supply for the transponder chip, out of the induced voltage of the *H*-field alternating at the Continuous Wave (CW) 13.56 MHz operating carrier frequency, emitted by the PCD antenna.

A. The Proximity Coupling Device (PCD), the reader

In the equivalent circuit of fig. 1, V_{PA} is the driver source of the NFC chip, which generates a square-wave carrier frequency signal, e.g. of 5 $V_{(PP)}$ amplitude, by switching the output between the positive supply voltage and ground (GND). R_{PA} represents the driver output resistance. Depending on chip type, R_{PA} may have 2 … 5 Ohms. The two branches of the differential network which connects the PCD antenna to the driver output are identical. The reason to have two branches instead of just one is a practical one: the supply is limited to low voltages, and the R_{ON}-resistance of the driver switches cannot be neglected. The differential output allows to have an output voltage of almost twice the supply, and thus to reduce the power losses in the output driver. Furthermore, a differential driver stage due to compensation always means a better noise suppression for the rest of the circuit. So the total output power V_{PA} is split up into two sources $V_{PA}/2$, which drive the output signal in phase opposition.

Fig. 2 shows the driver schematic, driver output with appendent switching states and the "Break before Make" function. Two drivers are built identically, each one connected to V_{SUP} via a switch on one side and to *GND* via a switch on the other side. The driver output resistance R_{PA} mentioned above is a characteristic of every switching path. There are three possible combinations of switching states: *I*, *II* and *BbM* ("Break before Make"). In state *I*, switches S_{1HI} and S_{2LO} are closed, whereas S_{2HI} and S_{1LO} are open.

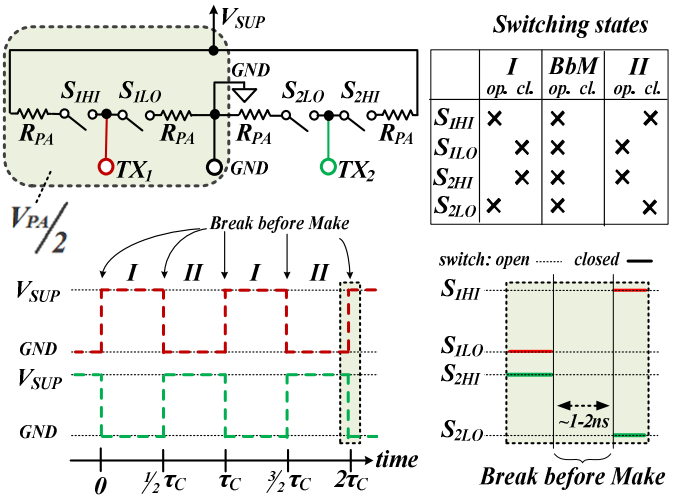

Fig. 2. Driver schematic (top left), switching states(top right), driver output (bottom left) and "Break before Make" (bottom right).

So output TX_1 is high (= V_{SUP}), while TX_2 is low (= *GND*). State *II* is the very reverse. To protect the drivers from short circuit currents (as there are unavoidable fabrication tolerances in switching times of individual switches), states *I* and *II* do not change directly, but have a transition state called "Break before Make" which lasts for only about 1 – 2 ns. In this state all switches are open to prevent a short between V_{SUP} and *GND*. The output signals of both drivers are plotted bottom left in fig. 2. The output on TX_1 is in red, the one on TX_2 in green colour. The time axis of the driver output diagram is divided into units of $\frac{1}{2}\tau_C$, which is half a driver carrier period, as τ_C is equal to $1/f_c$ with f_c = 13.56 MHz.

Each branch of the reader network consists of an EMC filter, which is a simple LC low-pass, to convert the square-wave carrier into a sine-wave signal of low harmonic distortion. A narrow-band impedance adjustment network, simply called "matching network", is the next stage. It transforms the antenna impedance Z_{ANT} into a different impedance Z_{IN}. The PCD loop antenna is a complex, inductive load. At the carrier frequency and modulation bandwidth Z_{ANT} can be represented well by the parallel resonant circuit of antenna inductance L_{ANT}, parasitic antenna capacitance C_{ANT}, and conductor resistance R_{ANT}. In case the *Q*-factor of the antenna is too high and would have significant impact on the modulation bandwidth, an external resistance R_Q is added in series.

B. The Proximity Integrated Circuit Card (PICC), the transponder

Inductive coupling connects the reader with the transponder, which is typically in an NFC tag or a Proximity Smartcard, via their loop antennas. The behavior of a Proximity Integrated Circuit Card can be emulated with a parallel resonant circuit, as it is shown in fig. 1, composed by the antenna's inductance L_{TP}, the impedance adjustment network capacitor C_{TP} and R_{TP} as *Q*-damping resistor. The parasitic capacitance and resistance of the antenna can be neglected regarding the much larger values of C_{TP} and R_{TP}. Whereas L_{TP} is an antenna parameter, the value of C_{TP} can be

chosen to get the desired resonant frequency. The bridge rectifier transforms the sinusoidal signal to DC-voltage, as supply for the transponder chip.

The coupling as parameter is represented by the mutual inductance *M*, or the coupling coefficient *k,* which is affected by the distance between the two coaxial antenna loops.

III. NETWORK ANALYSIS

A. *Simplification of the Network*

The differential network structure of the reader can easily be transformed into an equivalent single ended network structure of equal behaviour. Fig. 3 shows how components have to be transformed in general. The left hand side of the figure represents the differential structure, the right hand side is single ended.

If we consider the serial circuit, impedances at the sine-wave angular frequency ω are given by $Z = R$ for resistance, $Z = j\omega L$ for inductance and $Z = 1/j\omega C$ for capacitance. For the total impedance all parts are added. For the conversion of differential to single-ended, two impedances *2 Z* must be represented by one impedance *1 Z*. This means for the resistance, $2 \cdot (R/2) = 1 \cdot R$, for inductance $2 \cdot (j\omega L/2) = 1 \cdot (j\omega L)$ and for capacitance $2 \cdot (1/j\omega 2C) = 1 \cdot (1/j\omega C)$.

Whereas resistance and inductance values for the differential to single-ended conversion of the serial circuit have to be multiplied by two, the capacitance value has to be divided by two.

A similar consideration holds for the parallel circuit. The total admittance $Y = 1/Z$ is given by the sum of the individual admittances. The admittance is given by $Y = 1/R$ for resistance, $Y = 1/j\omega L$ for inductance, and $Y = j\omega C$ for capacitance. Two admittances *2 Y* have to be represented by one *1 Y*. Using this analogy, the differential network from fig. 1 is now simplified to a single ended network, which is shown in fig. 4. All the components of the signal branch between V_{PA} and the antenna are transformed, so the conditions stay the same, compared to the differential structure.

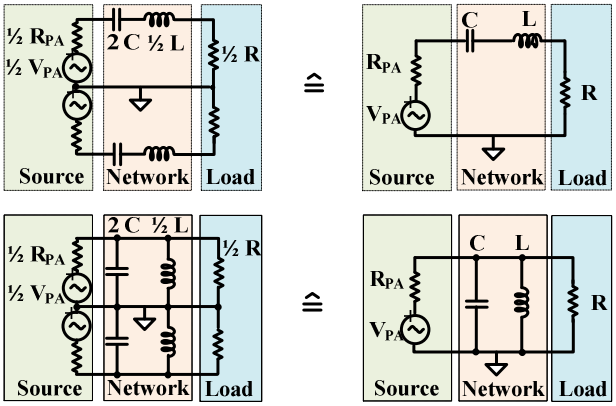

Fig. 3. Single-ended to differential network conversion for serial (top) and parallel (bottom) LCR network.

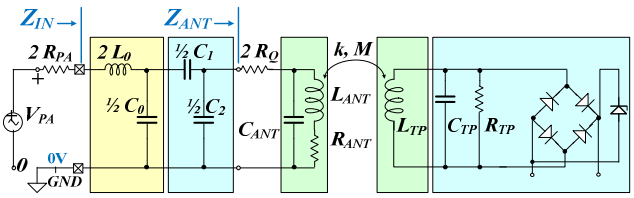

Fig. 4. Single-ended representation of the NFC coupling network.

The single ended source $V_{PA}/2$ is now doubled to $V_{PA\ (0,+)}$. The antenna equivalent circuit element values remain the same. The "matching network input impedance" Z_{IN} is considered as the impedance which can be measured between TX_1 and TX_2 of fig. 1 and will be equal to the impedance measured between *TX* and *GND* of fig. 4. Typical practical values for the desired real impedance are 20 … 100 Ω. The input should be real, to avoid problems like voltage peaks during the amplifier switching states described above.

B. *Linearize the System: calculate the PICC-limiting resistor*

A standard approach to solve the system of fig. 4 involves time domain simulations, which are lengthy and do not provide much insight. In fact since the circuit contains non linear elements (such as diodes) it cannot be solved algebraically unless some simplifying assumptions are made.

Here we assume that the combination of rectifier and limiter can be seen as a variable resistor R_{TP}, as shown in fig. 5 that achieves one of two goals:

(1) keep the voltage at the rectifier input at a predefined amplitude level (ideal limiter behavior).
(2) keep the average power dissipated by R_{TP} equal to the actual power dissipated by rectifier, limiter and either digital parts of a transponder chip, or the variable resistor of a Ref. PICC at DC side.

Both methods require a Thevenin Equivalent of the circuit of fig. 4 up to the rectifier input with R_{TP} disconnected, which results in an open circuit voltage V_{OC} and a series impedance $Z_{OUT,RTP} = R_0 + j\,X_0$.

The second method is basically numerical and requires a measurement to identify the relation $I_{NLE}(V_{NLE})$ of the non linear element, but is more accurate in representing reality.

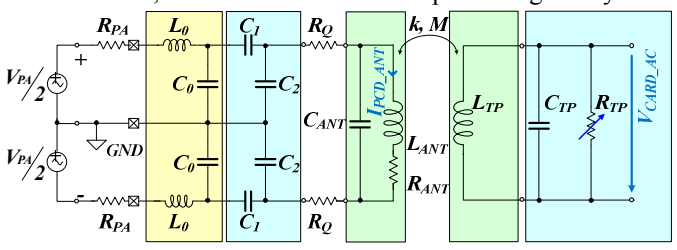

Fig. 5. Rectifier and limiter replaced by a variable resistor R_{TP}.

The solution is then obtained by equating the voltages V_{NLE} with $V_{CARD\text{-}AC}$ and the current $I_{NLE}(V_{NLE})$ to $I_{CARD\text{-}AC}$; this provides a working point for the amplitudes V_W, I_W from which we can derive $R_{TP} = V_W/I_W$. The first method is much simpler and requires solving a voltage divider with one real impedance and a complex one. The solution to this is

$$R_{TP} = \frac{BR_0 + \sqrt{B(R_0^2 + (1-B)X_0^2)}}{1-B}; \quad B \equiv \frac{V^2_{LIM}}{V^2_{OC}} \qquad (1)$$

where V_{LIM} is the limiter voltage amplitude at the rectifier input, and R_0,X_0 the components of $Z_{OUT,RTP}$ mentioned above. With our assumption of a variable resistor modeling the limiter, we do not take into account the squaring of the signal at the rectifier input, but we do account for the limiter operation in keeping the voltage amplitude at the rectifier input close to constant or exactly constant. Even more importantly, we have linearized the circuit, enabling linear analysis in the Laplace domain, or complex frequency domain, using $s = \sigma + j\,\omega$.

C. Equation System

The single ended network (slightly simplified by neglecting R_{PA} and R_Q) can be illustrated with a Transformed Transponder Impedance Z_{TTI} [3 - 5], representing the transponder and its influence on the reader. Based on fig. 6, starting on the right hand side, the network equations can be formulated. To reduce the complexity of the equations, Laplace transformation is used.

$$u = L \cdot \frac{di}{dt} \rightarrow Z_L(s) = s \cdot L \qquad (2)$$

$$u = \frac{1}{C}\int i dt \rightarrow Z_C(s) = \frac{1}{s \cdot C} \qquad (3)$$

The Laplace domain allows simple terms for capacitive and inductive impedance, see equations (2) and (3). Resistive impedance stays the same as it is in time domain, as it is a constant.

The network equations are:

$$Z_{TP}(s) = s \cdot L_{TP} + \frac{R_{TP}}{1 + R_{TP} \cdot C_{TP} \cdot s} \qquad (4)$$

Z_{TP} stands for the total impedance of the transponder. Coupling and feedback of the transponder to the reader are put together in the Transformed Transponder Impedance Z_{TTI} [3].

$$Z_{TTI}(s) = -\frac{k^2 \cdot s^2 \cdot L_{ANT} \cdot L_{TP}}{Z_{TP}} \qquad (5)$$

$$Z_{ANT,TTI}(s) = \frac{R_{ANT} + s \cdot L_{ANT} + Z_{TTI}}{1 + s \cdot C_{ANT}(R_{ANT} + s \cdot L_{ANT} + Z_{TTI})} \qquad (6)$$

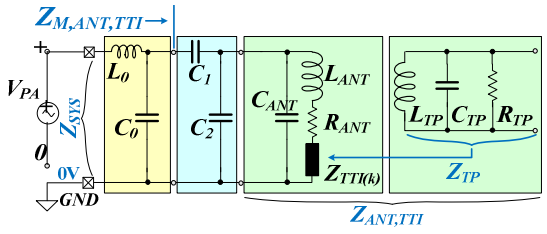

Fig. 6. PCD network extended by Transformed Transponder Impedance.

It is instructive to derive a more explicit dependency of Z_{ANT} from R_{TP} and k. Upon substituting (5) into (6) we get:

$$Z_{ANT,TTI}(s) = \frac{R_{ANT} + \alpha(k, R_{TP}) \cdot s \cdot L_{ANT}}{1 + s \cdot C_{ANT}(R_{ANT} + \alpha(k, R_{TP}) \cdot s \cdot L_{ANT})} \qquad (7)$$

$$\alpha(k, R_{TP}) \cdot = (1 - k^2) + k^2 \frac{R_{TP}}{R_{TP} + L_{TP} \cdot s + C_{TP} L_{TP} R_{TP} \cdot s^2} \qquad (8)$$

Equation (7) shows that coupling affects the antenna inductance by a complex gain factor α given in (8). If the transponder is tuned to the carrier frequency we can substitute $C_{TP}\,L_{TP} = -1/s^2$ obtaining:

$$\alpha(k, R_{TP}) \cdot \cong (1 - k^2) + k^2 \frac{R_{TP}}{L_{TP} \cdot s} \qquad (9)$$

Equation (9), exact for a tuned card, can be shown to be a good approximation as long as the card detuning is small compared to its bandwidth $Q_{TP} << \omega_0^2 / |\omega_0^2 - \omega_C^2|$, i.e. $|\omega_0 - \omega_C| << \omega_0 / (2 \cdot Q_{TP})$, where ω_C is the carrier frequency, ω_0 the card resonance frequency and $Q_{TP} = R_{TP}/(\omega_c\, L_{TP})$ the card quality factor. Such assumption is typically true at close coupling where the limiter ensures a low value for Q_{TP}. If we focus on the series branch of the antenna impedance, i.e. the numerator in (7), and use the approximation in (9) we obtain

$$Z_{ANT,TTI,SERIES}(s) \cong (1 - k^2) s \cdot L_{ANT} + R_{ANT} + k^2 \frac{L_{ANT}}{L_{TP}} R_{TP} \qquad (10)$$

From eq. (10) we see that coupling tends to reduce the original L_{ANT} value by a factor (1-k^2) and to increase R_{ANT} by an amount equal to $k^2\, R_{TP}$ (L_{ANT}/L_{TP}.). Both terms are responsible for the reduction in quality factor of the reader due to proximity of the card. Simulations showed that despite R_{TP} decreases with increasing k, the resistive term is an increasing function of k.

The antenna impedance $Z_{ANT,TTI}$ in (6) is adapted by the matching network C_1,C_2 to $Z_{M,ANT,TTI}$

$$Z_{M,ANT,TTI}(s) = \frac{1}{s \cdot C_1} + \frac{1}{\frac{1}{Z_{ANT,TTI}} + s \cdot C_2} \qquad (11)$$

Combining the equations leads to the total network impedance Z_{SYS}

$$Z_{SYS}(s) = s \cdot L_0 + \frac{1}{\frac{1}{Z_{M,ANT,TTI(s)}} + s \cdot C_0} \qquad (12)$$

Since we are interested in the energy transfer between reader and transponder only at the carrier f_C at steady state, it is worth considering the equations in frequency domain just at that frequency. So we can replace the Laplace parameter s by $j\omega_C$ to get a suitable solution in all equations (4-12).

D. Calculating the Values for the Matching Network, and finally the Antenna Current

Under usual conditions all circuit component values are given, except for C_1 and C_2, which are combined to a narrow-band impedance adjustment to transform $Z_{ANT,TTI}$ to $Z_{M,ANT,TTI}$ and except for R_{TP}, which limits the supply voltage V_{CARD} of the transponder chip. We will see that for a desired target impedance, which depends on the desired field strength, there is at most a unique solution.

Starting with R_{TP} it has to be mentioned, that V_{CARD} physically varies with the coupling conditions, but has to be limited to a certain supply voltage for the chip. So R_{TP} serves as a limiting resistor, whose value depends on the coupling ($R_{TP}(k)$) and therefore it is no constant in fact. To keep the

calculation simple, R_{TP} is still assumed as a constant anyhow on the first step and in equations (9) – (10). R_{TP} is part of $Z_{ANT,TTI}$ as shown in equations (4) – (6).

The values of the Matching Network can be extracted from Z_{SYS}. Solving the equation for C_1, C_2 gives

$$C_1 = \frac{1}{j \cdot \omega \cdot \left(\frac{1}{\frac{1}{Z_{ANT,TTI}} + j \cdot \omega \cdot C_2} + Z_{M,ANT,TTI} \right)} \quad (13)$$

and

$$C_2 = \frac{\frac{1}{Z_{ANT,TTI}} + \frac{1}{Z_{M,ANT,TTI} + \frac{1}{j \cdot \omega \cdot C_1}}}{j \cdot \omega} \quad (14)$$

with $Z_{M,ANT,TTI}$ the matching impedance that needs to be seen at the left of the matching network to achieve an input impedance equal to the desired resistance R_M is given by

$$Z_{M,ANT,TTI} = \frac{R_M - j\omega \cdot L_0}{1 + j\omega \cdot C_0 (j\omega \cdot L_0 - R_M)} \quad (15)$$

Equations (13) and (14) are complex and need to be considered as pair of equations each, for the real and imaginary part. An analytic solution for the general case is possible but due to its complexity the solution is best achieved numerically. It can be shown, however, that if there is a solution to the matching problem, such solution is unique. Let's consider a simplified case, namely when the EMC filter is absent, i.e. $L_0 = C_0 = 0$. In this case $Z_{M,ANT,TTI} = R_M$. The solution is then given by:

$$C_2 = \frac{R_m - R_A}{\omega \sqrt{R_A R_m \cdot (R_A^2 + X_A^2 - R_A R_m)} + \omega \cdot R_m X_A} \quad (16)$$

$$C_1 = \frac{R_A}{\omega \sqrt{R_A R_m \cdot (R_A^2 + X_A^2 - R_A R_m)}} \quad (17)$$

where $R_A + jX_A = Z_{ANT,TTI}$ depends on the coupling condition via k and R_{TP} (7,8,10). It is worth noting from eq. (16) that matching is only possible if $R_M > R_A$, i.e. that an antenna resistance cannot be matched via capacitors to a smaller resistance than itself.

Once the values of C_1 and C_2 are changed to their new values that achieve matched impedance, the voltage across R_{TP} which was calculated with different values for C_1 and C_2 will no longer equal the limiter amplitude voltage discussed in Section B. A new value for R_{TP} should then be calculated, which in turn worsens the matching of C_1 andC_2 via eq. (7), (16)-(17). All three, C_1, C_2 and R_{TP} can be calculated in a loop, until both the matching constraint and the limiter voltage constraint are met.

Once the circuit components are all fixed, including the mutual inductance (e.g. via a von Neumann integral [6]), we can solve the circuit by considering a unit voltage supply V_{PA} and calculating the current on the reader coil with linear equations. The admittance transfer $H_{Y,I\text{-}ANT} = I_{ANT}/V_{PA}$ will then define the channel transfer from Power amplifier (PA) voltage to antenna coil, and therefore to air interface alternating H-field. Such transfer function will be a 7th order one for the circuit of fig. 5, i.e. it is characterized by 7 poles. This function can be represented in Matlab with the Laplace domain coefficients of its numerator and denominator. In this way the frequency response can be evaluated by observing $s = j\omega$, and the effect of coupling onto channel detuning can be easily simulated.

A second transfer function is also very useful, namely the voltage transfer $H_{V,PICC} = V_{CARD\text{-}AC}/V_{PA}$ from PA voltage to PICC voltage, taken at the rectifier input. Such transfer has exactly the same poles as $H_{Y,I\text{-}ANT}$, but different zeros, therefore the frequency response will also differ. Typically at far coupling distance the effect of the PICC quality factor is visible mostly in $H_{V,PICC}$ but not in $H_{Y,I\text{-}ANT}$.

By analyzing the pole locus on the Laplace plane one can visualize how the mutual induction interaction modifies the channel properties. For instance a reader pole at the carrier frequency $|s| = \omega_C$ indicates a tuned channel. At closer coupling the poles of the card become more and more damped by action of the limiter; such load on the reader reduces in turn its quality factor, and tends to move it away from its resonance frequency. By adjustment of C_1 and C_2 one can compensate this effect and keep the impedance adjusted and the channel tuned at different coupling distances.

IV. Simulation of an NFC coupling scenario

A. Reader with NFC35 Antenna and EMC-Filter, ISO/IEC Ref. PICC Class 1

To show the capabilities for the analytical NFC coupling network model in a practical use case, we investigate a coupling scenario of two loop antennas over varied distance. The NFC antenna on reader side is a 35 x 35 mm 4-turn loop antenna etched on FR4 as described in [7] (air coil), the antenna on transponder side is the ISO/IEC10373-6 Reference PICC Class 1 [2]. The Ref. PICC is adjusted to 13.56 MHz resonance frequency, and the resistor is adjusted for every position such that 3 VDC can be measured. The distance of the coaxial loop antennas is varied from 80 mm (nearly no influence) to a minimum of 3 mm. We differentiate 2 cases and present the same diagrams on 2 pages: 1st case is the NFC coupling network with EMC filter, as shown in fig. 8, 2nd case is the NFC network without EMC filter, as shown in fig. 14. The PCD parameters used in simulation are reported in Table I.

The traces for the antenna impedance Z_{ANT} (blue) and the network impedance Z_{IN} are shown in the Smith Chart of fig. 7 and 13, at the operating frequency 13.56 MHz. We indicate also the region for antenna impedances which can be adjusted to the desired 50 Ω by our impedance adjustment network structure using C_1 and C_2.

TABLE I. Values for the simulated NFC coupling network

V_{PA}	R_{PA}	R_M	R_Q	R_{ANT}	L_{ANT}
5 V	1 Ω	50 Ω	0.53 Ω	6.6 Ω	1.83 µH
distance: 80...3 mm		***L_0***	***C_0***	***C_1 fix***	***C_2 fix***
with EMC		560 µH	226 pF	31 pF	106 pF
without EMC		0	0	59 pF	75 pF

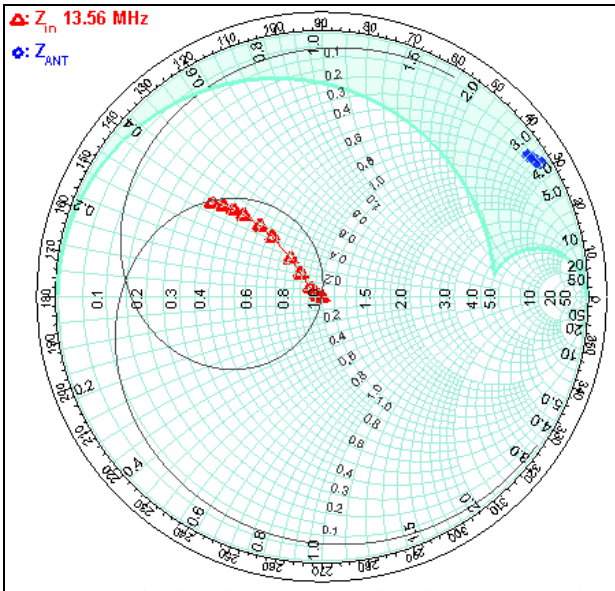

Fig. 7. Smith Chart showing antenna impedance and network impedance at 13.56 MHz for fix capacitor values over varied coupling distance.

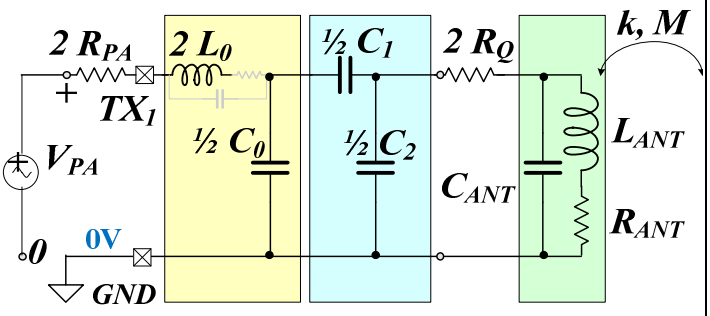

Fig. 8. Schematics of the modeled NFC coupling network.

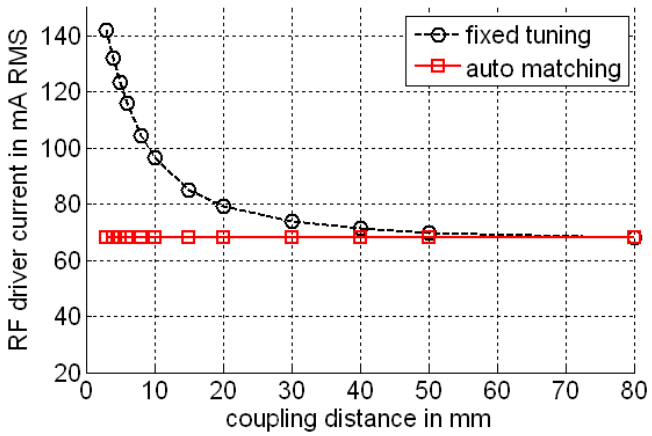

Fig. 9. RF driver current over varied coupling distance.

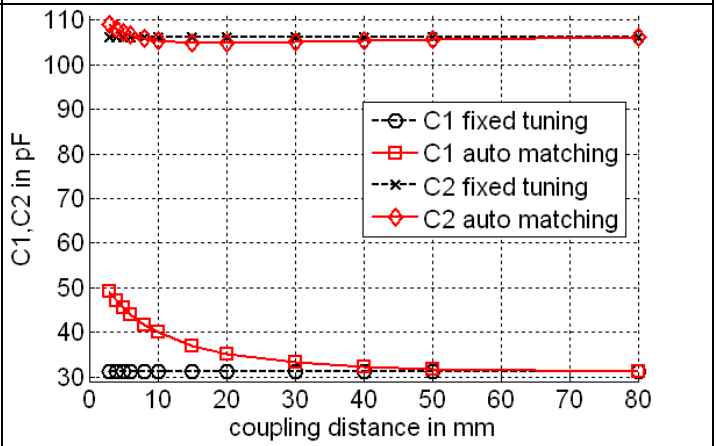

Fig. 10. Capacitor values for fixed and adjusted impedance over varied coupling distance.

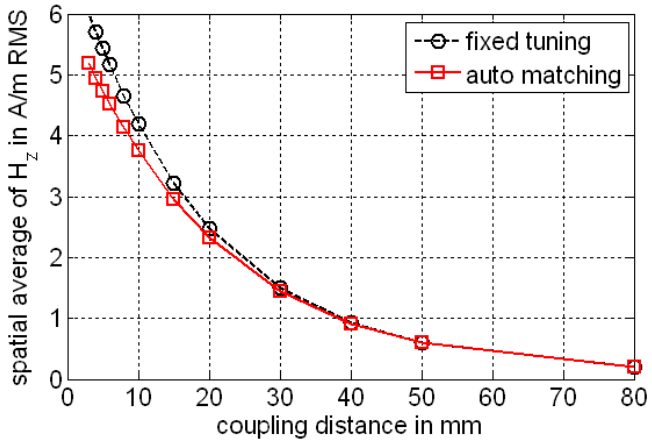

Fig. 11. Uniform equivalent *H*-field on the Ref. PICC over coupling distance.

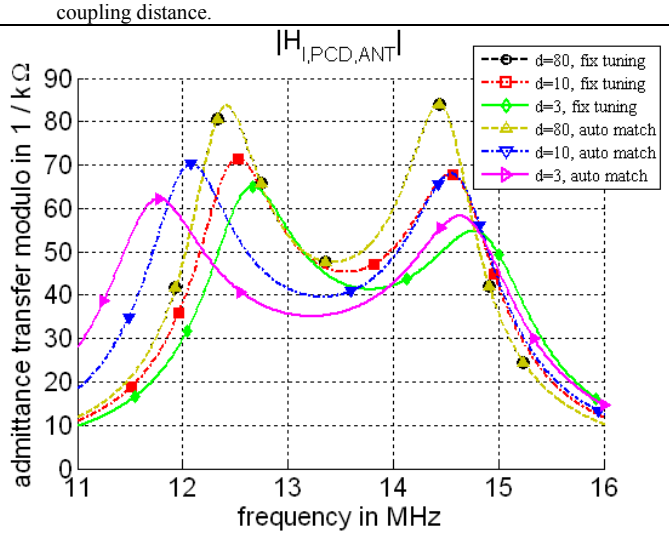

Fig. 12. Reader antenna admittance over frequency, for selected coupling distances.

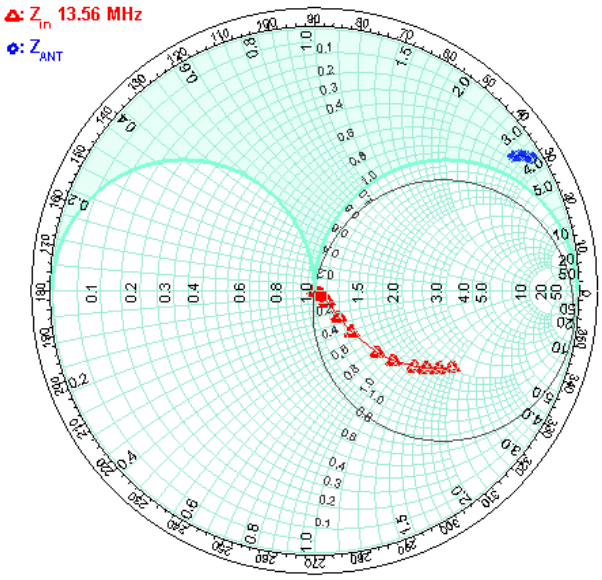

Fig. 13. Smith Chart showing antenna impedance and network impedance at 13.56 MHz for fix capacitor values over varied coupling distance.

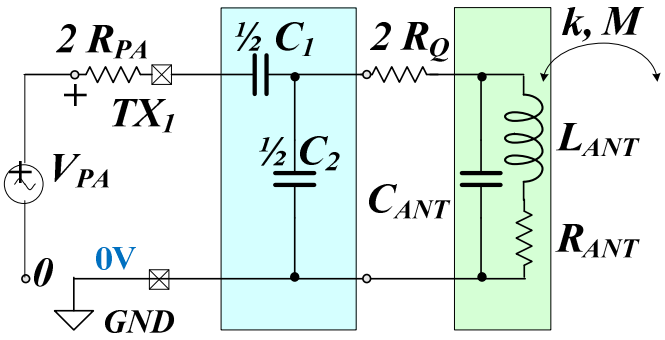

Fig. 14. Schematics of the modeled NFC coupling network.

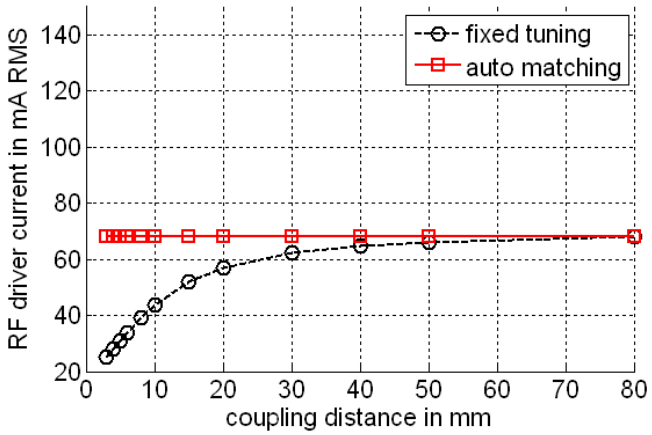

Fig. 15. RF driver current over varied coupling distance.

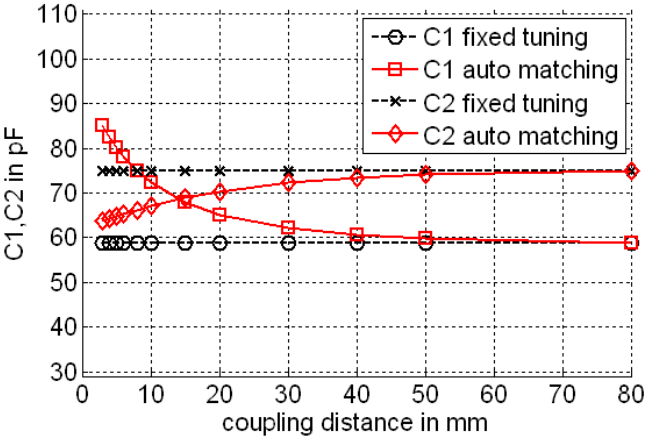

Fig. 16. Capacitor values for fixed and adjusted impedance over varied coupling distance.

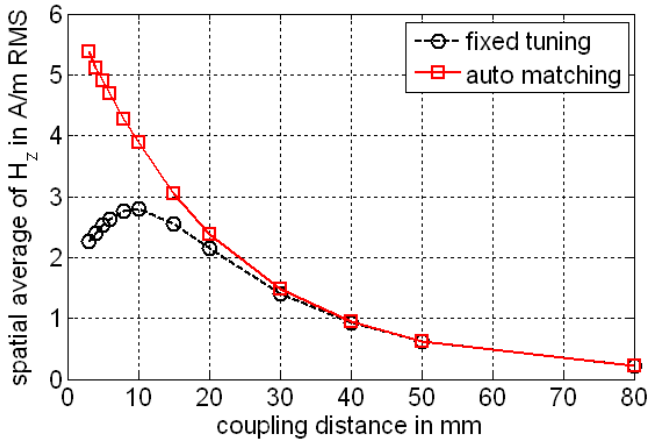

Fig. 17. Uniform equivalent *H*-field on the Ref. PICC over coupling distance.

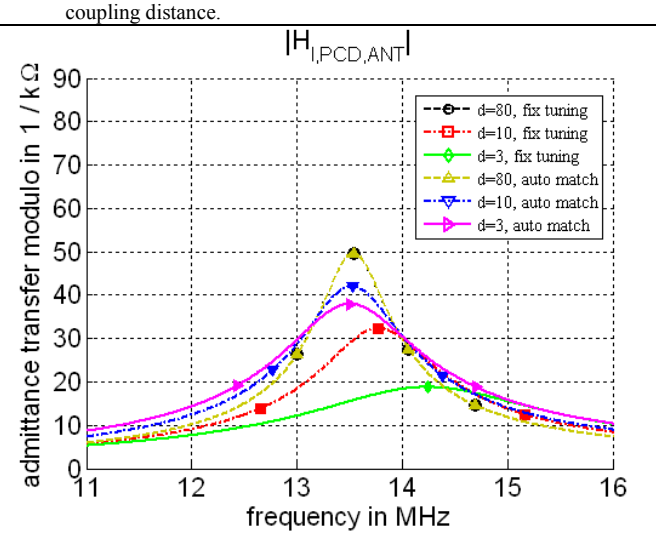

Fig. 18. Reader antenna admittance over frequency, for selected coupling distances.

As can be seen, with EMC filter the impedance decreases with reduced distance of the PICC antenna to the NFC antenna. This means, the RF current to be provided by the amplifier shown in fig. 2 increases towards zero distance, which is potentially unsafe, requires a protection mechanism or a large margin. Moreover, Z_{IN} becomes complex. Without EMC filter, as shown in fig. 13 the impedance increases with coupling. Since the voltage output of the amplifier is constant, the RF current drops down at reduced distance (fig. 15) which makes it difficult to feed RF power into the antenna. This impact on the NFC antenna inductance by the varied mutual inductance can be compensated by adjustment of C_1 and C_2, so that the impedance remains at the intended R_M, which here is 50 Ω. The required capacitance values for this "auto-matching" case are shown in fig. 9 and 15. As the comparison of fig. 9 and 15 shows, the RF current is constant into constant 50 Ω over coupling in this case, and the RF power is equal with or without EMC filter. Fig. 11 and 17 show the available, spatially averaged alternating *H*-field over distance, measured in coaxial orientation over the PICC antenna surface.

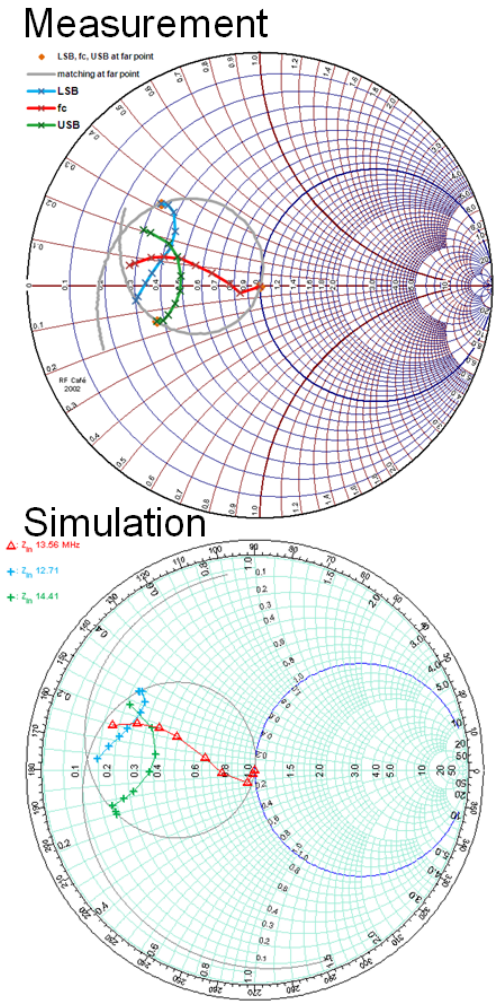

Fig. 19. Comparison between simulation and measurement results for the network input impedance at the carrier (red), the upper (green) and lower (blue) side band frequency for the coupling of two NFC antennas over distance.

A comparison of a similar coupling scenario was made between simulation and a real measurement, using an Impedance Analyzer. Results, shown in fig. 19 indicate very similar traces for impedances at carrier frequency (fC), Lower and Upper Sideband (LSB = 15/16 fC, USB = 17/16 fC).

V. Conclusions

We have considered an analytic network model for contactless HF Near Field Communication. Starting with an original, complete, differential network we have shown how to simplify this to the relevant parts of a single-ended circuit model of equal properties, which we have modelled by complex network calculation. Relevant parts such as the EMC filter, an impedance adjustment network, the loop antenna representation and the impact of close coupling to a contactless transponder have been discussed. Using our model, we have investigated the impedance at the operating frequency, RF amplifier power, contactless power transmission, the communication channel and a method to compensate the impact of variable card loading by impedance adjustment. As the relevant Standards specify properties at the air interface, such a model is useful to estimate the behaviour of a complete NFC solution, based on NFC chip properties like RF power, the impedance adjustment network and the NFC antenna. A brief comparison to measurements proofs our approach valid.

References

[1] NFC Forum (www.nfc-forum.org/specs/), NFC Analogue Specification, Revision Draft 0.38, June 2011.

[2] ISO/IEC 10373-6:2011(E), Identification cards – Test methods – Part 6: Proximity Cards. ISO, Geneva, Switzerland, 2011.

[3] K. Finkenzeller, *RFID-Handbuch: Grundlagen und praktische Anwendungen von Transpondern, kontaktlosen Chipkarten und NFC,* 6. Edition Carl Hanser Verlag GmbH & Co. KG, Mai 2012.

[4] M. Gebhart, J. Bruckbauer, M. Gossar, „Chip Impedance Characterization for Contactless Proximity Personal Cards", 7th CSNDSP, pp. 826 – 830, July 2010, Newcastle, UK.

[5] R. Stadlmair, M. Gebhart, "Cadence Simulation Environment for contactless near-field communication tags", 11th Int. Conf. on Tel., pp. 39 – 46, ISBN 978-1-61284-169-4, June 2011, Graz, Austria.

[6] F. E. Neumann, "Allgemeine Gesetze der inducirten elektrischen Ströme", Abhandlungen der Königlichen Akademie der Wissenschaften zu Berlin, Seiten 1 – 87, 1845.

[7] M. Gebhart, T. Baier, M. Faccini, "Automated Antenna Impedance adjustment for NFC", to be published in ConTEL, Zagreb, June 2013.

[8] H. Witschnig, E. Sonnleitner, J. Bruckbauer, E. Merlin, „Eigenvalue analysis of close coupled 13.56 MHz RFID labels", Int. Microwave Symposium (IEEE MTT-S), pp. 324 – 327, June 2006.

[9] U. Muehlmann, M. Gebhart, M. Wobak, „Mutual Coupling Modeling of NFC Antennas by Using Open-Source CAD/FEM Tools", 3rd Conf. on RFID TA, Nov. 2012, Nice, France.

[10] D. Seebacher, M. Gebhart, M. Stark, „Measurement Instrument Selection for Very High Bit Rate Contactless Transponder evaluation", 2nd Conf. on RFID TA, pp. 140 – 147, ISBN 978-1-4577-0028-6, Sept. 2011, Sitges, Spain.

[11] J. Langer, M. Roland, "Anwendungen und Technik von Near Field Communication (NFC)", ISBN 978-3-642-05496-9, Springer, 2010.

[12] H. C. Jing, „Capacity performance of an inductively coupled near field communication system", Antennas and Propagation Society Int. Symposium, pp. 1-4, July 2008.

[13] Y.-S. Chen, S.-Y. Chen, H.-J. Li, "Analysis of Antenna Coupling in Near-Field Communication Systems", Transactions on Antennas and Propagation, pp. 3327 - 3335 Vol. 58, Issue 10, Oct. 2010.